VERSITA

GEOCHRONOMETRIA 41(1) 2014: 15–23
DOI 10.2478/s13386-013-0119-4

Available online at
www.springerlink.com

OSL AND TL CHARACTERISTICS OF FINE GRAIN QUARTZ FROM MONGOLIAN PREHISTORIC POTTERY USED FOR DATING

SARAN SOLONGO[1, 2], DANIEL RICHTER[2], TUGULDUR BEGZJAV[1] and JEAN-JACQUES HUBLIN[2]
[1]*Institute of Physics and Technology, Mongolian Academy of Sciences, Enkhtaivnii urgun chuluu 54b, 13330 Ulaanbaatar, Mongolia*
[2]*Department of Human Evolution, Max-Planck-Institute for Evolutionary Anthropology, Deutscher Platz 6, Leipzig, Germany*

Received 29 August 2012 Accepted 27 June 2013

Abstract: The OSL, post-IR OSL and pulsed post-IR OSL applied to polymineral grains and calculated by fitting to the data the contributions from fast, medium and slow components revealed that the polymineral samples under study are dominated by the medium component. An increase in D_e's with increasing integration intervals was observed, which is considered as an indication of increasing medium and decayed fast component; and the equivalent doses obtained using different components or minerals reflect also the shape of the dose distributions. The identified fast component in polymineral sample has photoionization cross section of $1.2\pm0.02 \times 10^{-17}$ cm^2. The present study shows the usefulness of the application of different luminescence techniques combined with fitting procedures as a check which should be adopted in dating protocols. Based on luminescence ages obtained on polymineral grains from prehistoric pottery samples from the Boroo settlement, Mongolia, which are in agreement with independent age control by ^{14}C on charcoal material, it is argued that the manufacturing of Xiongnu – pottery at this site lasted until ca. 130±75 AD.

Keywords: polymineral fine grains, quartz, OSL, post-IR OSL, fitting OSL components.

1. INTRODUCTION

Studies of Optically Stimulated Luminescence (OSL) from heated brick (Bøtter-Jensen *et al.*, 2000) for retrospective dosimetry and from archaeological bricks/tiles (Solongo *et al.*, 2006; Bailiff, 2007; Solongo, 2008) for historical studies in the interpretation and reconstruction of building chronologies are focused on the precise dose evaluation in fired quartz. For the determination of the absorbed dose using Single-Aliquot Regenerative (SAR) procedures (Wintle and Murray, 2006) provide accurate estimates of the dose for quartz dominated by fast OSL component. However, if other components are large compared to the fast component, they can lead to inaccurate determination of D_e when the SAR protocol is applied. For samples with a weak fast OSL component, the thermal stability of the medium OSL component becomes important as it will contribute to the initial signal that is usually used for dating (Wintle and Murray, 2006).

For the determination of the absorbed dose in polymineral fine grains, illuminating the sample with IR light to remove the feldspar OSL signal before stimulating with shorter wavelengths is often used in an attempt to achieve a clean quartz OSL signal. Longer IR bleaching may remove most of feldspar contribution; however, a blue-stimulated feldspar OSL signal remains even after IR exposure; this

Corresponding author: S. Solongo
e-mail: saran@ipt.ac.mn

ISSN 1897-1695 (online), 1733-8387 (print)

Springer

signal can overlap with the quartz OSL. Thus, the possibility to deplete the OSL signal from feldspars prior to stimulation with blue diodes in order to obtain the quartz-dominated post-IR OSL-signal from polymineral grains was proposed by Banerjee *et al.* (2001) and termed double-SAR method. Another approach to reduce the feldspar OSL signal is elevated temperature IR bleaching, e.g. at 220°C (Jain *et al.*, 2003); however, prolonged IR bleaching at 220°C also depletes the quartz OSL. Another possible instrumental method for isolating a quartz signal from a mixed quartz-feldspar sample is pulsed optical stimulation (Denby *et al.*, 2006). Using pulsing, it is possible to observe a quartz dominated signal from a polymineral sample by measuring the OSL after most of the feldspar signal has decayed.

The objective of this work is to investigate the potential of applying the OSL, post-IR OSL stimulation and pulsed stimulation techniques to estimate the dose in polymineral samples. The influence of blue and infrared stimulation on the TL curves is examined. The OSL, post-IR OSL and pulsed post-IR OSL decay curves are analyzed and compared.

2. MATERIALS

Samples

All ceramic samples originate from an archaeological site at the Xiongnu settlement of Boroo (48°45'20"N, 106°16'57"E), Mongolia – traditionally dated according to the written sources between 200 BC and AD 155 (Dorjsuren, 1961). Evidence of several pit habitations was found and thousands of artifacts have been excavated. Based on independent radiocarbon dates of charcoal material from the Boroo settlement, it is found that it was occupied from the end of the 2nd century BC to the beginning of the 1st century AD. Radiocarbon dates of charred material recovered from pits of the Xiongnu period sites at the Boroo settlement (calibrations performed using Oxcal v3.10) were provided by Ramseyer *et al.* (2009).

Sample's mineral composition

The mineralogical composition of the polymineral fine grain samples were analysed by X-ray diffractometry (XRD). Semi-quantitative analysis was performed using the Rietveld method and the results show that all polymineral samples contain quartz as the major mineral but different feldspar minerals such as sodium aluminium silicate (albite), potassium aluminium silicate (microcline) and potassium aluminium silicate hydrate (muscovite).

Additionally, bulk chemical analyses were performed by spectrometry of X-ray fluorescence, results of both methods (**Tables 1** and **2)** suggest that samples are clearly more dominated by quartz. Samples Hu3-2 and Hu5-1 contain more similar numbers of K- and Na-feldspar grains than sample Hu4-1 which contains ~71% of quartz.

3. METHODS

For luminescence procedures, the outer layer of the ceramic fragments was removed and the obtained cores were carefully crushed in a hydraulic press and sieved. All crushed material was subjected to 15% and 30% H_2O_2 to remove organic material and to 10% HCl to dissolve carbonate minerals. No quartz coarse grain material was available after HF etching, but few Na-feldspar remained. The 4-10 μm fine grains were separated and deposited onto discs (ca. 1 mg per aliquot) for OSL and TL measurements.

Due to the small sample sizes, dose rate determinations were performed by the analysis of U, Th and K concentrations using neutron activation analysis (NAA) on about 200 mg of crushed sample (<160 μm). Dose rates for samples were calculated from the nuclide concentrations using the conversion factors of Adamiec and Aitken (1998). The correct estimation of the moisture content is one of the most influential parameters of the dose rate estimate. The 'as is' moisture of the potsherds was measured (1-1.5%), but since the excavation they had been stored for 2 years. The depth of ~1 m of overburden sediment (no sediment material was available) for the entire burial period was estimated and the samples at the manufacturing centre were assumed to be surrounded by other potsherds.

All OSL and TL measurements were performed using an automated Risø TL/OSL-DA-20 reader, equipped with blue light-emitting diodes emitting light at 470±20 nm (2.6 eV) and IR diodes emitting at 870 nm. The blue and IR stimulations deliver ~50 mW cm^{-2} and ~135 mW cm^{-2} at the sample position, respectively (Bøtter-Jensen *et al.*, 2003), and 90% of their full powers were used for stimulation. Laboratory irradiation was undertaken using a calibrated ^{90}Sr/^{90}Y beta sources delivering (0.224 Gy/s) to fine-grain aliquots. The IRSL and blue stimulated OSL signals were detected after passing through three 2.5 mm thick U-340 Hoya filters (290-370 nm). For TL measurements D410 transmission filters (410±30 nm) were employed.

For dose determination SAR and post-IR-OSL method protocol were employed using a preheat at 260°C for 10 s for natural and regenerative dose and a cut-heat at 220°C for test dose measurements. According to the post-IR OSL SAR, an infra-red stimulation (IR) is inserted prior to blue stimulation to obtain the post-IR OSL signal from polymineral grain; IR stimulation for 60 s was done at 50°C. Regenerative doses were 4.48, 8.95, 13.43, 0 and 4.48 Gy and a test dose of 1.12 Gy was given to a single aliquot. TL regenerated dose measurements were tested on few samples. The SAR protocol was applied for D_e determination to 12 aliquots of each sample (limited by the available sample material). Additionally, pulsed measurements using the Risø attachment to the DA-20 reader, the LEDs were pulsed with 40 μs on-time and

150 μs off-time (Denby *et al.*, 2006) and the OSL signal was only recorded during the off-time.

4. RESULTS AND DISCUSSION

OSL, post IR OSL and pulsed OSL results

To illustrate some of the luminescence characteristics of polymineral samples under study a representative blue stimulated OSL and post-IR OSL decay curves of sample Hu4-1 are shown in **Fig. 1a** and 1**b**. According to the post-IR OSL, the infrared stimulation prior to OSL measurement should reduce the feldspar signal and the subsequent post-IR OSL should be obtained almost exclusively from contributions of quartz fine grains. As can be seen from the figure, the blue stimulated OSL and post-IR OSL curves are very similar in intensity; and the IR signal before the blue-stimulated OSL indicated that quartz fine grains dominate the sample. The ratio between IR and blue OSL signal for natural doses was 1:50. The weak IR signal which was stimulated at 50°C is shown in **Fig. 1d**.

To check whether the obtained OSL signal originates from quartz only, the blue stimulated OSL decay curves were fitted with a sum of exponential components (fast, medium and slow). The relative contributions of the exponential components to the total OSL obtained for the initial 10 s as a function of stimulation time of the sample Hu4-1 are shown as inset of **Fig. 1a**. Here F denotes the fast component of the blue stimulated OSL, M – medium of the blue stimulated OSL and S represents the slow component plus background; F+M denotes the sum of fast and medium components. It was observed that the initial blue stimulated OSL is dominated by the fast and medium components which contribute ~80% in the initial 2 s. The fast component has decayed by the end of 1.2 s and the medium component is dominant in the time range from 1.5 to 6 s. For stimulation times over 7 s, only the slow component is visible and it is represented over this time scale as a constant signal.

The post-IR OSL signal is shown in **Fig. 1b**; all components seem to be depleted by IR exposure in similar manner. The first 3 channels of the post-IR OSL signal is also dominated by the fast and medium components and the fast component makes up to 60% and medium component up 40% of the initial post IR-OSL signal. It has to be stated, that all components – fast, medium and slow – are recovered in post-IR OSL signal, where the infrared stimulations prior to blue stimulated OSL measurement were carried out at a temperature of 50°C. As can be seen from **Fig. 1**, following 10 s IR stimulation at 50°C does not effectively deplete both feldspar signal and post-IR OSL signal and the magnitudes of the OSL components were affected slightly.

For pulsed post-IR-OSL signal detection, 40 μs on and 150 μs off time were employed, where the OSL signal was recorded during the off-time. **Fig. 1c** shows the pulsed post-IR OSL decay curve of sample Hu4-1; an 87% reduction in the initial intensity is observed; it was assumed that the feldspar signal, which was not reduced by a prior IR bleaching, has been effectively removed using stimulation pulses. However, the pulsed post-IR OSL signal is apparently lacking a fast component (see **Table 2**). Assuming that only feldspar and quartz minerals are present in this polymineral sample, and that a complete IR depletion of the feldspar component was not registered in post-IR OSL signal, it was initially suggested that the fast component detected is associated with feldspar. The pulsed post-IR OSL protocol attempts to cut-off the mixed mineral signal from that by feldspars; fitting procedures revealed that due to the pulsing mode the subsequent OSL decay had only medium and slow components left. When using 40 μs on and 150 μs off time which were employed for pulsed post-IR-OSL signal detection it might deplete much more OSL signal from quartz. The fast component which was not pronounced in our samples was in fact removed in pulsed OSL signal.

Table 1. *Semi-quantitative analysis of minerals in the polymineral samples obtained from XRD.*

Sample	Quantity (%)			
	Quartz	Albite	Microcline	Muscovite
Hu3-2	61.1	13.5	13.6	11.8
Hu4-1	71.5	9.0	9.6	9.9
Hu5-1	57.1	8.9	15.7	18.4

Table 2. *Chemical composition from X-ray fluorescence of the samples Hu3-2, Hu4-1 and Hu5-1.*

	SiO_2 (%)	Al_2O_3	Fe_2O_3	TiO_2	MnO	MgO	CaO	Na_2O	K_2O	P_2O_5
Hu3-2	60.715	16.610	6.770	0.814	0.093	2.360	2.644	1.530	2.495	0.296
Hu4-1	62.680	16.900	7.000	0.822	0.075	2.160	1.654	1.530	2.416	0.179
Hu5-1	63.380	16.490	6.690	0.798	0.076	2.190	2.017	1.680	2.887	0.308

	Ba(ppm)	Sr	Ce	Co	Cr	Cu	La	Ni	Rb	Pb	Zr
Hu3-2	689	320	87	27	152	34	32	43	107	22	221
Hu4-1	678	233	82	26	176	24	32	45	112	28	221
Hu5-1	558	283	96	20	129	46	46	40	121	30	241

Note: Analyses are given in weight percentages for major and minor elements, and in ppm for trace elements.

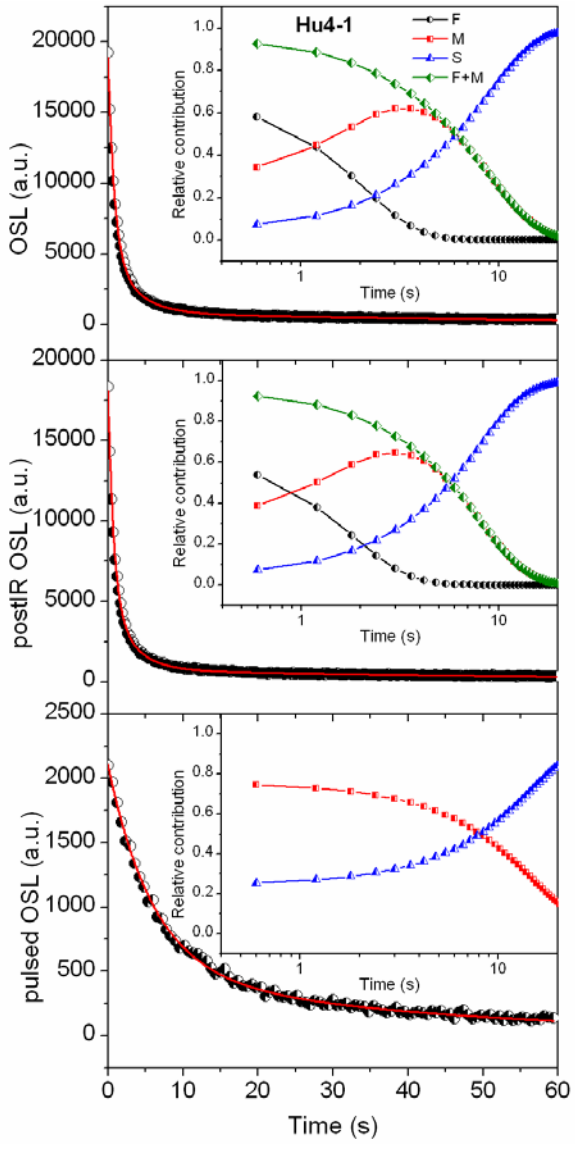

Fig. 1. *Representative decay curves of polymineral sample Hu4-1 a) blue-stimulated OSL at 125°C; b) post-IR- OSL following IR stimulation at 50°C; c) pulsed post-IR-OSL 125°C. Inset: relative contribution from different exponential components (fast, medium and slow) to the total blue stimulated OSL are plotted against the stimulation time components. F: fast component; M: medium; S: slow component of blue stimulated OSL; F+M: the sum of fast and medium components.*

To demonstrate that SAR protocols used here are applicable to these samples the contributions of different OSL components to the D_e's obtained were checked. To estimate the magnitude and decay rate of the fast and medium OSL components, the final OSL, post-IR OSL and pulsed post IR-OSL data were fitted to a sum of first-order exponential components (c.f. Bailey *et al.*,2011) using Microcal Origin 8.0, running a Levenberg-Marquardt algorithm (in each case iterated until the results were fully stabilized). The results of fitting multi-exponential functions to derive the magnitude n_i, decay rate f and photo-ionization cross section σ_i of the fast, medium OSL components and of the slow component plus background signal obtained as a mean value of 10 independent fittings are given in **Table 3**.

To investigate this further, CW-OSL decay curve of sample Hu3-1 is shown in **Fig. 3a**. The different OSL components of the signal obtained for the initial 10 s of the decay curve are shown in the inset of **Fig. 3a** on a semi-logarithmic plot. The contributions from different components calculated by fitting to the data the sum of exponential equations revealed that for sample shown in **Fig. 3**, the fast component makes up about 50% of the initial signal, the medium component about 40% and the slow component plus background about 10%. It was observed that the fast component has decayed by the end of 1 s and the initial signal is dominated by the medium component from 0.7 to 6 s. For stimulation times longer than 7 s, only the slow component is visible and it is represented over this time scale as a constant signal.

Bulur (2000) suggested that the CW-OSL decay curve can be mathematically converted into an equivalent LM-OSL data set termed 'pseudo-LM-OSL'. These curves are considered reliable for separating the fast and medium components using mathematical deconvolution. **Fig. 3b** shows such pseudo-LM-OSL curves obtained using the CW-OSL decay from **Fig. 3a**. The parameters of fitting to the CW-OSL and LM-OSL curves are presented in **Table 3**, where the magnitudes and photoionization cross sections of each component found to be consistent with each other. Sample Hu5-1 was analyzed in a similar way. The parameters of fitting the CW-OSL curves for samples Hu3-2 and Hu5-1 are summarized in **Table 3**.

The fitting results suggest that fast, medium and slow components come from both feldspar and quartz. The photoionization cross section obtained for the medium component in these polymineral samples are in the range from $(2.11\text{-}3.1)\times10^{-18}$ cm^2. The photoionization cross section for the fast component in the polymineral grains was $1.2\pm0.02\times10^{-17}$ cm^2.

TL results

To further investigate the behaviour of the luminescence from the polymineral samples under study here, regenerative thermoluminescence (TL) test measurements were carried out. Representative natural and regenerative TL curves after beta irradiation followed by preheating at 70°C, all measured on the same aliquot, are shown for sample Hu3-2 in **Fig. 2**. The natural TL glow curve exhibits maxima at about 260-280°C and 320-340°C. The regenerated doses were 6.7 Gy, 8.9 Gy and 11.2 Gy. The regenerated TL signal shows low temperature TL peaks at approximately 110 and 150°C, and a prominent high temperature peak at ~250°C with a shoulder at ~340°C. The equivalent dose of 7.8±0.3 Gy determined for the plateau between 300°C and 360°C is also shown in **Fig. 2** (dots), and was determined from the regeneration growth curve by interpolation.

In order to illustrate the relative contribution of quartz and feldspar minerals in polymineral sample to the luminescence, the residual TL signals resulting from prior blue and IR stimulations were examined. These experiments are similar to those reported by Murray *et al.* (2009) using preheats at 90°C and 250°C and reflect the effect of various durations of IR stimulation on regenerated TL. **Fig. 4a** shows the influence of IR stimulation for 0, 4, 8, 16, 32, 64 and 128 s on the regenerated TL signal for preheat temperatures of 90°C using a single aliquot of Hu3-2. Infrared stimulation for 4 s reduces the TL over the entire temperature range; the prolonged stimulation

Table 3. *Parameters of magnitude (n) decay rate (f) of and photoionization cross sections (σ) of the OSL components (fast, medium and slow + background, respectively) derived for blue stimulation light, post-IR OSL and pulsed post-IR blue stimulation (470±30 nm)from polymineral sample Hu4-1, Hu3-2 and Hu5-1.*

Sample	Components	Magnitude n_i (a.u.)	Decay rate f_i (s^{-1})	Photoionization cross-section σ (cm^2)
Hu4-1, OSL	Fast	1.120e4±3.85e2	1.198±0.022	1.125e-17±2.106e-19
	Medium	1.581e4±3.14e2	0.291±0.012	2.732e-18±1.098e-19
	Slow	5.495e4±1.44e3	0.015±8e-4	1.456e-19±7.531e-21
Hu4-1, post-IR OSL	Fast	9.207e3±3.18e2	1.349±0.025	1.267e-17±2.346e-19
	Medium	1.442e4±2.57e2	0.338±0.011	3.170e-18±1.068e-19
	Slow	5.082e4±1.23e3	0.015±7e-4	1.428e-19±6.393e-21
Hu4-1, pulsed post-IROSL	Fast	-	-	-
	Medium	9.570e3±3.75e2	0.168±0.004	1.574e-18±4.245e-20
	Slow	2.038e4±3.04e2	0.024±0.001	2.309e-19±1.328e-20
Hu3-2, CW-OSL	Fast	1.033e4±2.15e2	1.243±0.016	1.167e-17±1.529e-19
	Medium	1.616e4±2.57e2	0.225±0.007	2.116e-18±6.576e-20
	Slow	4.761e4±6.07e2	0.016±0.0005	1.510e-19±4.617e-21
Hu3-2, PSEUDO-LM-OSL	Fast	1.451e4±3.37e2	-	0.791e-17±2.396e-19
	Medium	1.601e4±3.75e2	-	1.139e-18±4.810e-20
	Slow	4.929e4±3.94e2	-	1.074e-19±3.543e-21
Hu4-1, CW-OSL	Fast	1.242e4±2.54e2	1.306±0.016	1.226e-17±1.498e-19
	Medium	2.061e4±2.53e2	0.263±0.007	2.466e-18±6.154e-20
	Slow	5.133e4±5.66e2	0.018±0.0004	1.671e-19±4.257e-21
Hu4-1, PSEUDO-LM-OSL	Fast	1.919e4±3.78e2	-	0.778e-17±1.923e-19
	Medium	1.881e4±3.86e2	-	1.214e-18±4.548e-20
	Slow	5.246e4±2.74e3	-	1.152e-19±3.222e-21
Hu5-1, CW-OSL	Fast	9.910e3±2.15e2	1.313±0.017	1.233e-17±1.598e-19
	Medium	1.724e4±2.14e2	0.263±0.007	2.472e-18±6.225e-20
	Slow	4.822e4±4.99e2	0.017±0.0004	1.627e-19±3.849e-21
Hu5-1, PSEUDO-LM-OSL	Fast	1.590e4±3.12e2	-	0.755e-17±1.869e-19
	Medium	1.584e4±3.32e2	-	1.154e-18±4.417e-20
	Slow	4.949e4±1.48e3	-	1.126e-19±3.018e-21

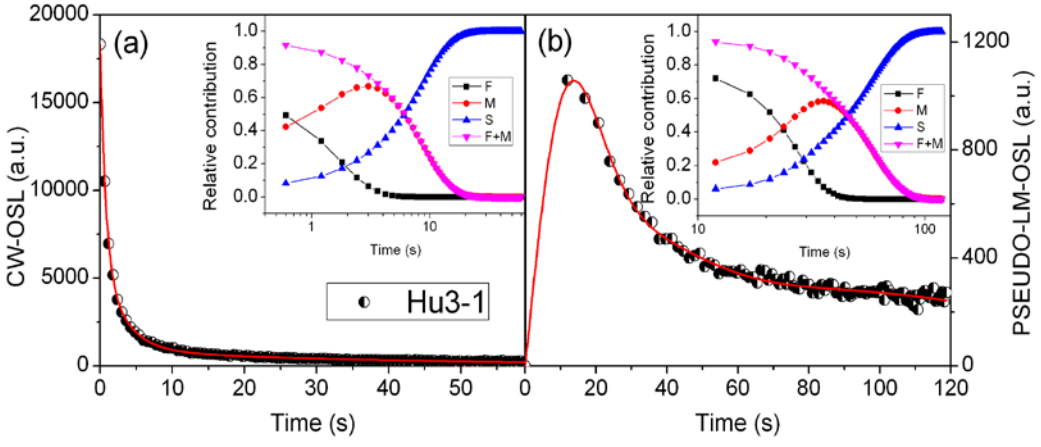

Fig. 2. *a) cw-OSL and b) pseudo LM-OSL curves obtained using transformation. Inset on a semi-logarithmic plot shows the contributions of the OSL components calculated by fitting to the data the sum of exponential equations.*

reduces low-temperature TL peaks around 150°C, which are most sensitive to stimulation with IR. In contrast, the TL signals are slightly affected by IR stimulation using TL signal for high-temperature preheat (**Fig. 4c**).

Fig. 4b shows the influence of blue OSL stimulation for 0, 4, 8, 16, 32, 64, and 128 s on the regenerated TL signal for preheat temperatures of 90°C using a single aliquot of Hu3-2. The observed TL peaks at 150°C, 250°C and 325°C are all reduced by OSL stimulation. The TL curves following a preheating of 250°C are shown in **Fig. 4d**. The 325°C TL peak is increasingly reduced with blue stimulation time between 4 and 128 s, while it is hardly affected by IR stimulation, suggesting that it is associated with the quartz OSL (e.g. Spooner, 1994)

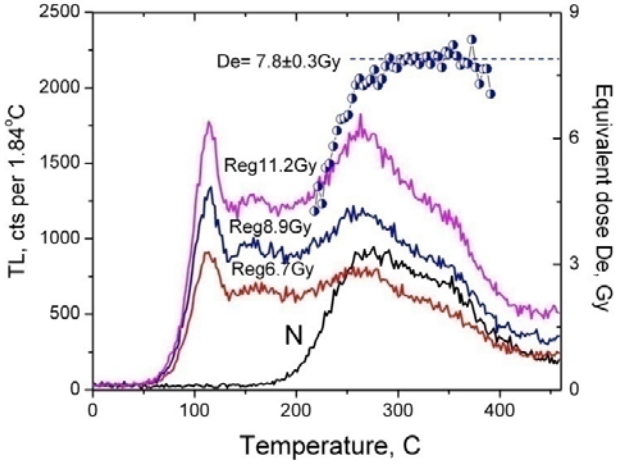

Fig. 3. *Natural as well as regenerated TL glow curves from one aliquot of sample Hu3-2 together with* D_e *over temperature obtained with a regeneration protocol.*

The weak IRSL signal measured at 50°C following a preheat at 250°C for 60 s probably derived from TL traps around 150°C. We infer that the OSL and post-IR OSL signals in our samples are related mostly to the traps between 300 and 360°C. These observations are in agreement with the previous measurements using OSL, post-IR OSL using preheat 260°C.

Luminescence ages

Fig. 5 shows the representative natural, regenerated and test dose OSL decay curves and corresponding dose response plots for two polymineral samples Hu3-2 (**Figs. 5a**, **b**, **c**) and Hu4-1 (**Figs. 5d**, **e**, **f**). We observed differences in the growth curves of both samples which were related to the different contributions of slow components.

The dose estimate D_e =7.13±0.24 Gy for sample Hu3-2 was estimated if the first 3 channels (=1.2 s) of the

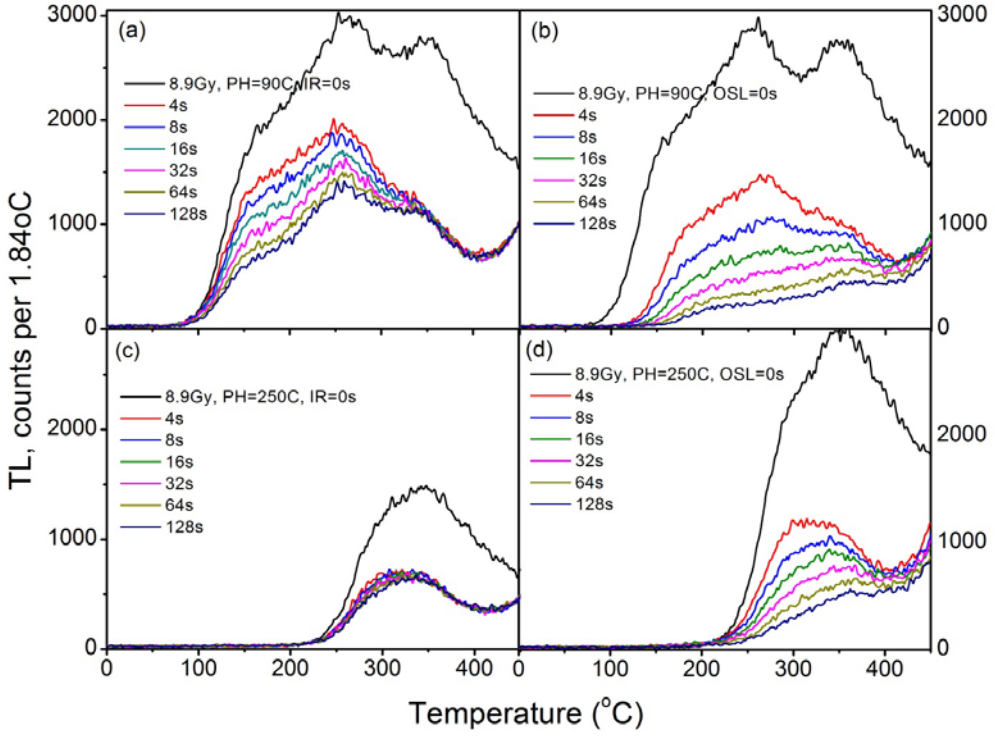

Fig. 4. *Influence of blue and IR stimulation on the TL signal of polymineral sample Hu3-2. A dose of 8.9 Gy was repeatedly given to four different single aliquots after measurement of its natural TL and preheated to (a, b) PH=90°C and (c, d) PH=260°C before measuring the TL curves. The measurements were repeated with optical stimulation for 4 s, 8 s, 16 s, 32 s, 64 s, 128 s to discriminate between the TL peaks which are sensitive to (a, c) infrared or (b, d) blue stimulation.*

Table 4. *Data for dose rate determination (using NAA) and equivalent doses (D_e), OSL and radiocarbon ages.*

Sample	U (ppm)	Th (ppm)	K (%)	Total dose rate (Gy/ka)	OSL D_e (Gy)	OSL age (a)	^{14}C age (cal BP)
Hu3-2	2.74±0.0292	12.7±0.0024	1.9353±0.0155	3.92±0.223	7.2±0.36 (n=12)	1837±75	1835±30 2100±35
Hu4-1	3.18±0.0220	12.3±0.0024	1.8713±0.0160	3.94±0.224	6.78±0.5 (n=13)	1720±90	2065±35 2255±30
Hu5-1	3.53±0.0170	15.3±0.0030	1.9669±0.0153	4.35±0.224	7.97±0.30 (n=12)	1830±110	2150±35

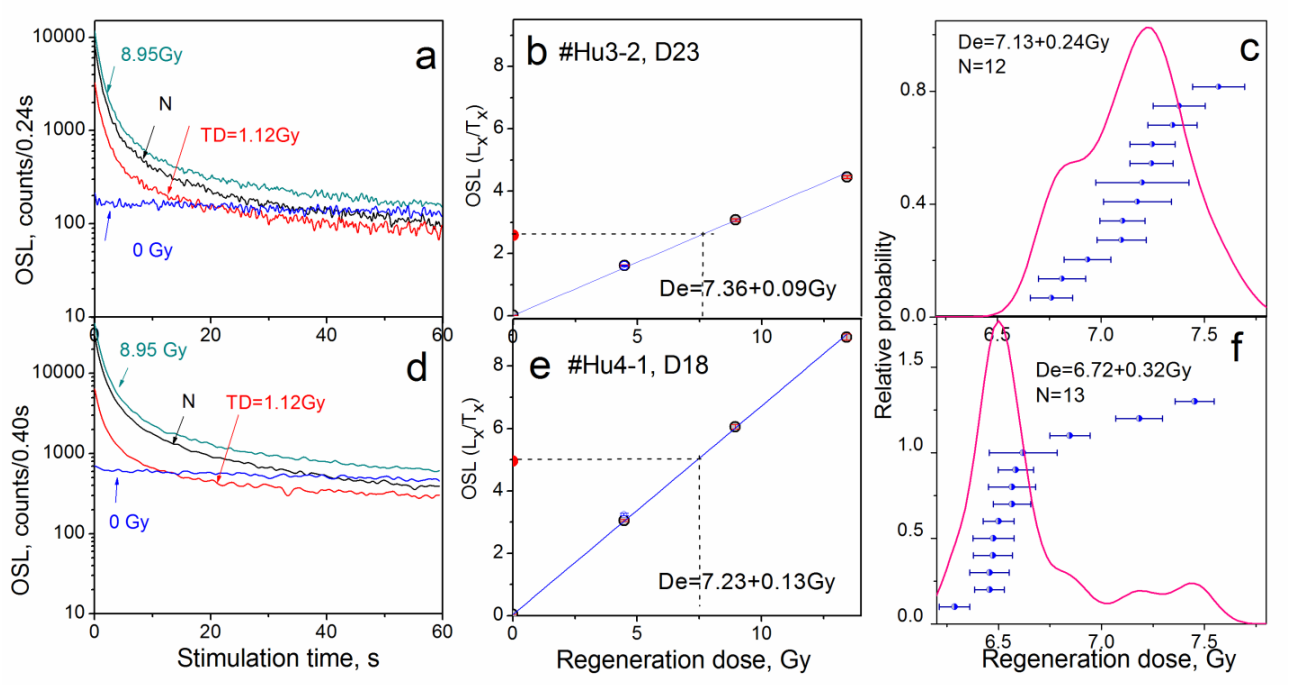

Fig. 5. *a), d) Natural, regenerated and test dose OSL decay curves for 60 s at 125°C; b), e) dose response curve and c), f) relative probability plot of* D_e *for polymineral samples Hu3-2 and Hu4-1.*

decay curve minus a background derived from the last 10 s was used for D_e calculations. Here the decay was dominant by the fast component. But the samples showed increasing D_e's with increasing integration periods, which is an indication of increasing medium component; for the time range (1-7 s) where the medium component is dominant, the dose estimate is D_e=7.66±0.30 Gy. The dose distributions are shown as a probability plot of D_e estimates in **Fig. 5d**; to illustrate it further the probability plots of D_e constructed using the following channels (1-3); (3-7); (8-12); (13-19) and (15-26) are shown (Fig. ii in the Appendix). For integration interval (8-12) where only the medium is active, the dose estimate is 7.66±0.30 Gy; for integration interval (13-19) D_e is 7.92±0.49 Gy for Hu3-2. In contrast, integration interval (8-12) for sample Hu4-1 is dominated by the medium component giving a dose estimate of 6.90±0.63 Gy and for integration (13-19) where the medium component is decaying the dose is 7.15±0.76 Gy (see Fig. ii in Appendix).

As can be seen from the figure, the dose distributions for sample Hu3-2 might be considered as result of two overlapping components, but for later time intervals the dose distribution shifts to higher doses.

For sample Hu4-1 we get a broader dose distribution and the mean 6.62±0.32 Gy for integration interval (0-1 s). We also observed an increase in D_e with increasing integration periods; but the overall shape did not change. Here we infer that the second population is due to the slow OSL components.

We assumed that the increase in D_e with integration integrals reflects the time ranges where individual OSL components will dominate. But a systematic, though not always significant, lower D_e for pulsed post-IR OSL is observed, which was evaluated on medium OSL component only, the fast component was deleted using 40 μs pulsing. Furthermore, for pulsed OSL measurements no increase in D_e with illumination time was observed.

The dose distribution might reflect the differences in mineralogical composition of our samples. We noticed that sample Hu4-1 contained much more quartz. Except for three larger doses, the dose distribution should be considered as a narrow one. This could be characteristically considered as quartz distribution. We obtained the higher doses from aliquots with showed relatively large slow component (see **Fig. 5d**, **e**, **f**) indicating that higher doses are obtained from slow components which might be related to feldspar.

In contrast, in case of Hu3-2 the mineralogical composition indicated relative larger amounts of different feldspars (microcline and albite). The dose distribution is relatively broad compared to those of sample Hu4-1 suggesting mixed doses obtained from both minerals. Another explanation would be: since the fast component decayed in sample Hu3-2 more quickly than in sample Hu4-1, it is suggested the dose estimates in Hu3-2 are mostly based on the medium component. The dose distributions may also indicate the beta dose rate uncertainties in samples: the feldspar-rich Hu3-2 sample shows much broader distribution then the quartz-rich sample Hu4-1.

The equivalent doses (D_e), dose-rate estimates and luminescence age results are summarized in **Table 4** together with radiocarbon ages from Ramseyer *et al.* (2009). The dose estimates are obtained using (3-7 channels) where the OSL signal is dominated by the medium component. Although the OSL age for sample Hu3-2 is in agreement with radiocarbon data, the OSL age for sample Hu4-1 and Hu5-1 are slightly younger than the calibrated ^{14}C ages. However the disagreement with radiocarbon data might be due to a different association or event dated with this technique. This is especially problematic because both pairs of radiocarbon data are significantly different for the same context.

5. CONCLUSIONS

To demonstrate that luminescence techniques such as OSL, post-IR OSL, TL and protocols used here are applicable to polymineral samples from pottery, the contributions of different OSL components to the D_e's obtained were checked. However, a fitting of the OSL and post-IR OSL of polymineral samples revealed different components which might come from feldspar and quartz. The OSL signal was dominated by the medium component with photoionization cross section of $(2.1\text{-}3.1)\times10^{-18}$ cm^2, and was observed for integration interval (1-6 s). The fast component identified for (0-1 s) had a photoionization cross section of $1.2\pm0.02\times10^{-17}$ cm^2. The increase in D_e was related to the decayed fast component; and the equivalent doses obtained using different components or minerals reflect also the shape of the dose distributions. Furthermore, the beta dose rate might be a reason for the dose distributions reflecting the differences in the mineralogical composition.

Prehistoric pottery samples from Xiongnu period pottery production centre at Boroo, Mongolia were subjected to different luminescence procedures involving attempts to separate the quartz and feldspar luminescence signal in polymineral samples. Luminescence ages agree in general with independent radiocarbon data as well as the age range provided by written sources for the archaeology of the Xiongnu period in Mongolia. It suggests that the manufacturing of Xiongnu – pottery at this site lasted until c. 130±75 AD.

ACKNOWLEDGEMENTS

Saran Solongo's research visit was financially supported by a grant from the DFG (German Research Foundation). Tsagaan Turbat, Institute of Archaeology, MAS is thanked for providing samples. We thank anonymous reviewers whose comments improved the paper significantly.

APPENDIX

Two figures are available as Supplementary Material in electronic version of this article at http://dx.doi.org/10.2478/s13386-013-0119-4. Fig. i.: XRD results of polymineral samples Hu3, Hu4-1, Hu5-1; Fig. ii.: Probability plots of sample Hu3-2, Hu4-1for integrating time intervals as indicated.

REFERENCES

Adamiec G and Aitken MJ, 1998. Dose-rate conversion factors: update. *Ancient TL* 16: 37-50.

Bailiff IK, 2007. Methodological developments in the luminescence dating of brick from English late medieval and post medieval buildings. *Archaeometry* 49(4): 827-851, DOI 10.1111/j.1475-4754.2007.00338.x.

Bailey RM, Yukihara EG and McKeever SWS, 2011. Separation of quartz optically stimulated luminescence components using green (525 nm) stimulation. *Radiation Measurements* 46(8): 646-648, DOI 10.1016/j.radmeas.2011.06.005.

Bøtter-Jensen L, Solongo S, Banerjee D, Murray AS and Jungner H, 2000. Using the OSL single-aliquot regenerative-dose protocol with quartz extracted from building materials in retrospective dosimetry. *Radiation Measurements* 32(5-6): 841-845, DOI 10.1016/S1350-4487(99)00278-4.

Bøtter-Jensen L, Andersen CE, Duller GAT and Murray AS, 2003. Developments in radiation, stimulation and observation facilities in luminescence measurements. *Radiation Measurements* 37(4-5): 535-541, DOI 10.1016/S1350-4487(03)00020-9.

Banerjee D, Murray AS, Bøtter-Jensen L and Lang A, 2001.Equivalent dose estimation using a single aliquot of polymineral fine grains. *Radiation Measurements* 33(1): 73-94, DOI 10.1016/S1350-4487(00)00101-3.

Bulur E, 2000. A simple transformation for converting CW-OSL curves to LM-OSL curves. *Radiation Measurements* 32(2): 141-145, DOI 10.1016/S1350-4487(99)00247-4.

Denby PM, Bøtter-Jensen L, Murray AS, Thomsen KJ and Moska P, 2006. Application of pulsed OSL to the separation of luminescence components from a mixed quartz/feldspar sample. *Radiation Measurements* 41(7-8): 774-779, DOI 10.1016/j.radmeas.2006.05.017.

Dorjsuren T, 1961. *Umard Khunnu [The northern Khunnu]*. Ulaanbaatar, Mongolian Academy of Sciences: (In Mongolian).

Jain M, Murray AS, and Bøtter-Jensen L, 2003. Characterisation of blue-light stimulated luminescence components in different quartz samples: implications for dose measurement. *Radiation Measurements* 37(4-5): 441-449, DOI 10.1016/S1350-4487(03)00052-0.

Murray AS, Buylaert JP, Thomsen KJ and Jain M, 2009. The effect of preheating on the IRSL signal from feldspar. *Radiation Measurements* 44(5-6): 1-6, DOI 10.1016/j.radmeas.2009.02.004.

Ramseyer D, Pousaz N and Turbat TS, 2009. The Xiongnu Settlement of Boroo Gol, Selenge Aimag, Mongolia. In: Bemmann J. eds, *Bonn Contributions to Asian Archaelogy, V4,* University of Bonn, Bonn: 231-240.

Solongo S, 2008. The luminescence dating of fired bricks from ancient Mongolian cities. In: Parzinger H, Bemmann J. eds, *Bonn Contributions to Asian Archaelogy, V4,* University of Bonn, Bonn: 593-596.

Solongo S, Wagner GA and Galbaatar T, 2006. The dose estimation using fast and medium components in fired quartz from archaeological site Kharakhorum, Mongolia. *Radiation Measurements* 41(7-8): 1001-1008, DOI 10.1016/j.radmeas.2006.05.023.

Spooner N, 1994. On the optical dating signal from quartz. *Radiation Measurements* 23(2-3): 593-600, DOI 10.1016/1350-4487(94)90105-8.

Wintle AG and Murray AS, 2006. A review of quartz optically stimulated luminescence characteristics and their relevance in single-aliquot regeneration dating protocols. *Radiation Measurements* 41(4): 369-391, DOI 10.1016/j.radmeas.2005.11.001.